arXiv:1605.03978v1 [physics.ins-det] 12 May 2016

Background Rejection of n^+ Surface Events in GERDA Phase II

Björn Lehnert[1]

Institut für Kern- und Teilchenphysik
Technische Universität Dresden, Germany

E-mail: bjoernlehnert@gmail.com

Abstract. The GERDA experiment searches for neutrinoless double beta ($0\nu\beta\beta$) decay in ^{76}Ge using an array of high purity germanium (HPGe) detectors immersed in liquid argon (LAr). Phase II of the experiment uses 30 new broad energy germanium (BEGe) detectors with superior pulse shape discrimination capabilities compared to the previously used semi-coaxial detector design. By far the largest background component for BEGe detectors in GERDA are n^+-surface events from ^{42}K β decays which are intrinsic in LAr. The β particles with up to 3.5 MeV can traverse the 0.5 to 0.9 mm thick electrode and deposit energy within the region of interest for the $0\nu\beta\beta$ decay. However, those events have particular pulse shape features allowing for a strong discrimination. The understanding and simulation of this background, showing a reduction by up to a factor 145 with pulse shape discrimination alone, is presented in this work.

1. Introduction

The Germanium Detector Array (GERDA) experiment [1] located at the Laboratory Nazionali del Gran Sasso (Italy) of INFN is searching for the $0\nu\beta\beta$ decay of ^{76}Ge. This isotope is embedded in HPGe detectors isotopically enriched to increase its fraction to about 87 %. An array of a few dozen HPGe detectors is immersed in a 64 m^3 tank filled wit LAr which serves as a cooling medium, an ultra pure passive radiation shield as well as an active scintillation veto in Phase II of the experiment. GERDA is proceeding in two phases: Phase I was completed in May 2013 with a Ge exposure of 21.6 kg·yr and a background level of 10^{-2} cts/(keV·kg·yr). This resulted in a half-life limit of $2.1 \cdot 10^{21}$ yr (90 % C.L) for the $0\nu\beta\beta$ decay [2]. The half-life of the SM allowed process of $2\nu\beta\beta$ decay was measured with increased precision as $(1.926 \pm 0.094) \cdot 10^{21}$ yr [3]. Phase II of the experiment is currently (fall 2015) commissioning, aiming to increase the exposure to more than 100 kg·yr and to reduce the background level further by more than one order of magnitude. The backbone of the background reduction are 30 newly produced broad energy germanium (BEGe) detectors which have superior pulse shape characteristics compared to Phase I semi-coaxial detectors [4].

The background analysis in Phase I [5] identified the major components of the background at $Q_{\beta\beta}$ for BEGe detectors as ^{42}K on the n^+ detector surface (59 %), ^{214}Bi and ^{228}Th in the detectors assembly (26 %), ^{42}K homogeneously in the LAr (6 %) and alpha emitters on the p^+ detector surface (3 %) in addition to other smaller contributions. The largest component of ^{42}K (Q_β=3525.4 keV, $T_{1/2}$=12.4 h) is part of the decay chain starting from ^{42}Ar (Q_β=599 keV,

[1] for the GERDA Collaboration

$T_{1/2}$=32.9 h) which is a trace isotope in natural argon. The high energetic electrons in the ^{42}K ground state transition (81.9 % probability) can mimic the $0\nu\beta\beta$ decay if it occurs close to the detector surface and if the electrons penetrate into the bulk detector volume. ^{42}K can be ionized after the ^{42}Ar decay and its attraction by the high voltage (HV) of the detectors was demonstrated. Additionally, ^{42}K concentrates on the n^+ detector surface [5, 6]. However, the electrons have to enter the detector volume passing through the n^+ electrode or the p^+ electrode which creates particular pulse shape features and enables a strong discrimination of these surface events. The understanding and simulation of the surface event discrimination will be shown in the following.

2. Pulse Shape Discrimination with BEGe Detectors

The GERDA BEGe detectors [7] are p-type HPGe detectors with an average mass of 670 g. The n^+ electrode is created with Li doping and covers around 98 % of the detector surface with a thickness of 0.5 to 0.9 mm. The p^+ electrode is created with B doping and has a thickness in the order of μm. When radiation creates electron-hole pairs, the charges are read out at the p^+ electrode with a charge sensitive pre-amplifier. The weighting field strength inside the detector is mostly constant throughout the bulk and increases sharply around the p^+ electrode. For energy depositions inside the bulk, the holes drift first towards the detector center and then towards the p^+ electrode due to a specific configuration of space charges. This results in the same charge trajectory in the volume with large weighting field strength and thus in the same pulse shapes for practically all bulk events [4, 8].

The experimental signature of the $0\nu\beta\beta$ decay in GERDA is a discrete deposition of $Q_{\beta\beta}$=2039 keV by the two final state electrons in a small volume of the bulk of the detector. Thus the majority of $0\nu\beta\beta$ events are single-site events (SSE) in the detector bulk which can be effectively distinguished from multi-site events (MSE) and surface events with the simple yet powerful pulse shape discriminator A/E [9]. The amplitude A of the current pulse is obtained after differentiation of the charge signal and 3-fold shaping with a 50 ns moving window average algorithm. After this soft shaping the current pulse still contains timing information of the charge collection. The energy E is obtained after significantly stronger shaping [10] which practically eliminates all timing information and results in an excellent energy resolution. The charge and current pulses of different event types are illustrated in Fig. 1. In case of MSE, multiple charge clusters arrive with a time offset due to different drift times. The amplitude and thus the A/E is reduced for these events. In p^+ events the holes and electrons drift simultaneously inside the large weighting field and thus immediately induce a higher current. Those events have a larger amplitude and thus a larger A/E value. In the n^+ electrode there is no electric field present

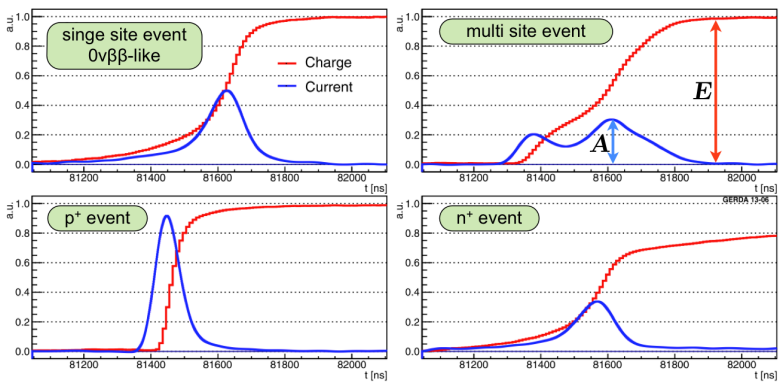

Figure 1. Charge pulse shape (red) and current pulse shape (blue) for interactions in BEGe detectors. Multi site events created by γ background, p^+ electrode events and n^+ electrode events created by surface background can be distinguished from bulk events created by $0\nu\beta\beta$ decay. Taken from [4]

and the dominant charge transport mechanism is diffusion. This results in two consequences: (1) The pulse formation is slower than for bulk events since the charges have to diffuse first into the region with electric field and (2) not all charges are collected resulting in a reduced energy measurement for interactions in a semi-active layer around the n^+ electrode.

The event characteristics of n^+ electrode interactions have been largely ignored in the past and the n^+ electrode was interpreted as a dead layer without charge collection. The dead layer interpretation, from now on called "old model" is valid for discrete energy depositions such as in gamma spectroscopy and $0\nu\beta\beta$ decay search. However, the semi-active layer is effectively reducing the n^+ electrode thickness (aka dead layer thickness) for surface events and significantly changing their measured energy. In addition, the active volume for processes with continuous energy deposition such as $2\nu\beta\beta$ decays is increased. The precise formation of those n^+ electrode "slow pulses" via diffusion is largely unknown and now studied with a "new model" of the n^+ electrode which can be folded into Geant4 Monte Carlo (MC) simulations via a post processing with pulse shape libraries. In the following, the new model is described, verified with calibration source measurements and applied to ^{42}K surface events and $2\nu\beta\beta$ decays in GERDA BEGe detectors.

3. New Model for n^+ Surface Events

The n^+ electrode of GERDA BEGe detectors is created with Li diffusion during a 2-4 h annealing cycle at 200 °C. The solution of the diffusion equation assuming a constant concentration on the surface is shown as the blue line in Fig. 2. The n^+ layer is divided into three regions according to the Li concentration profile [11]: (1) The fully active volume (FAV) in which charges drift in the electric field and are completely collected, (2) the drift dominated region (DDR) where no electric field is present and charges diffuse until they either reach the FAV or they reach the (3) recombination dominated region (RDR) where the charges recombine with a certain probability over time. The boundaries of these regions are constructed from first principles and measurements and are individual for each BEGe detector.

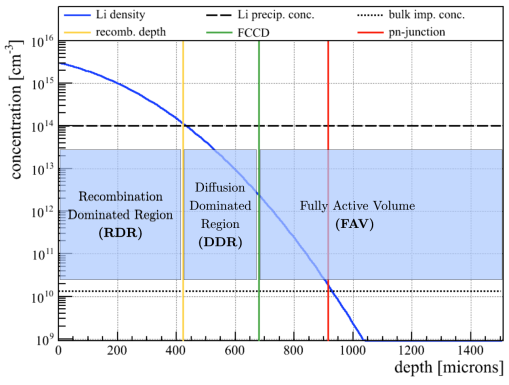

Figure 2. In the model the n^+ electrode is separated into three regions according to the Li concentration profile.

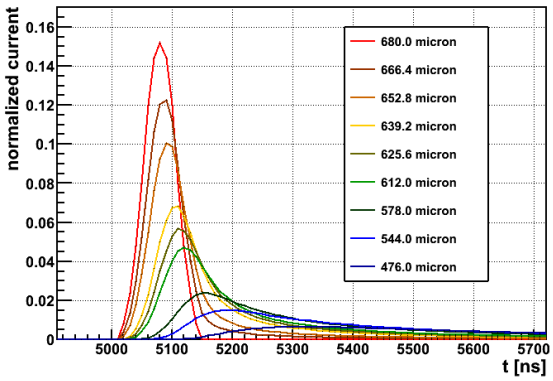

Figure 3. Simulated current pulses for different interaction depths in the n^+ electrode of a typical detector with 680 micron FCCD.

The p-n junction depth is defined where the Li donor concentration is equal to the bulk acceptor concentration. When the detector is biased and its bulk volume is fully depleted of free charge carriers, the number of charges in the bulk region compensate the same number of charges in the n^+ electrode creating a depletion zone which is equivalent to the FAV. The border of the depletion zone defines the full charge collection depth (FCCD). Due to the steep Li concentration profile, the FCCD is only $\mathcal{O}(100\,\mu\text{m})$ above the p-n junction. After the annealing

at high temperature, the Li concentration is supersaturated at room and LAr temperatures in the outer layers of the n^+ electrode. The Li forms precipitation centers which are electrically inert and believed to be responsible for charge recombination [11]. The recombination depth defined as the boundary between DDR and RDR is taken at a Li concentration of $10^{14}\,\mathrm{cm}^{-3}$ (see Ref. [13] for details). The FCCD is measured for each GERDA detector [12, 13] and used to recursively determine the Li concentration profile and the other region boundaries.

In these regions charges are simulated with the diffusion equation in a 1 ns time and 10 μm spatial dimension. Charges passing the FCCD entering the FAV are collected and form the current pulse. Charges passing into the RDR recombine with a probability of $0.002\,\mathrm{ns}^{-1}$. This value was determined when comparing different recombination rates with calibration data [13]. A model with zero recombination rate as well as a model with immediate recombination is strongly disfavoured by the data. Charges starting at a given depth below the surface result in very different pulse shapes which are collected in a pulse shape library depending on the interaction depth. Example pulses are shown in Fig. 3. The amplitude and the integral charge are reduced the more shallow the interaction. This surface interaction pulse shape library is combined with a bulk pulse shape library created with a modified version of ADL [14]. Geant4 simulations with the MaGe framework [15] are post processed with these two libraries such that the A/E information is extracted for an event based on the superposition of the individual pulse traces for each Geant4 hit in the event [13]. The MC simulations with the post processing of the new n^+ model are validated with ^{228}Th, ^{241}Am, ^{90}Sr calibration source measurements. The low A/E values of ^{208}Tl γ-lines and the single escape peak at 2103.5 keV are almost exclusively created by MSE effects. On the other hand, the low A/E values of the ^{241}Am 59.5 keV γ-ray are almost exclusively created by the n^+ electrode. The low A/E events of the ^{90}Sr source are created by betas being influenced by the n^+ electrode and by MSE effects from hard Bremsstrahlung. This beta source is taken as a proxy for ^{42}K decays in GERDA. The data of these calibration sources with different event topologies is well described by the MC simulations. For details see Ref. [13].

4. Application to Signal and Background Processes in GERDA Phase II

The new model is applied to simulations of ^{42}K decays in the LAr around a typical GERDA detector with 0.68 mm FCCD. The A/E versus energy spectrum is shown in Fig. 4 in which SSE in the bulk are normalized to $A/E = 1$. The following features can be seen: The γ-line at 1525 keV (18 % probability) has high and low A/E values coming from interactions close to the p^+ electrode and MSE interactions, respectively. The Compton region below the γ-line

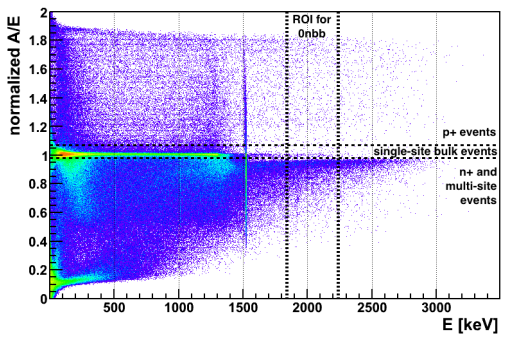

Figure 4. A/E versus energy of simulated ^{42}K events in LAr around a BEGe detector.

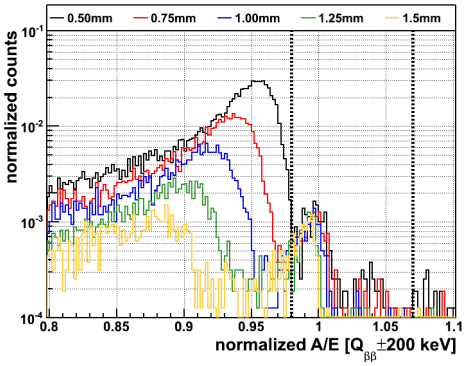

Figure 5. A/E in $Q_{\beta\beta}\pm200$ keV for simulated ^{42}K events around BEGe detectors with different FCCD.

is dominated by SSE interactions. The region above the peak, especially in $Q_{\beta\beta} \pm 200$ keV illustrated with vertical dashed lines, is dominated by interactions of electrons passing through the n^+ electrode. A part of their energy is deposited in the semi-active layer thus shifting the A/E for this population collectively into a band below the SSE bulk value of $A/E = 1$. The A/E values for these events are shown in Fig. 5 for various detectors with different FCCD. The gap between the SSE band and the slow pulse band and thus the discrimination possibility for n^+ surface events is larger for detectors with thicker n^+ electrode. Surviving events in the SSE region are due to Bremsstrahlung γ-rays jumping the n^+ electrode and depositing energy solely in the bulk. In this energy region a ^{42}K suppression of 45 can be reached with a cut of $0.98 < \mathrm{A/E} < 1.07$. The suppressed energy spectrum of ^{42}K is shown in Fig. 6 (green) compared to the unsuppressed spectrum (red). The semi-active layer increases the number of events around $Q_{\beta\beta}$ by 35 % which can be seen in the comparison with the old model (black) in the residual plot. The suppression is further increased by the LAr scintillation veto by more than a factor of 3 for BEGe detectors. For ^{42}K events directly on the n^+ electrode there is less chance to create a Bremsstrahlung γ-ray without also depositing energy in the n^+ electrode and consequently reducing the A/E value of the event. The suppression in this case is up to a factor 145 with the same A/E cut. However, for these events the LAr veto is not effective since the beta is directly entering the detector without depositing energy in the LAr [13].

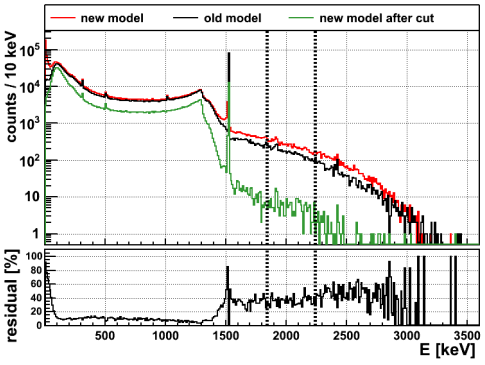

Figure 6. Spectrum of simulated ^{42}K events for the new model, old model, and the new model after A/E cut.

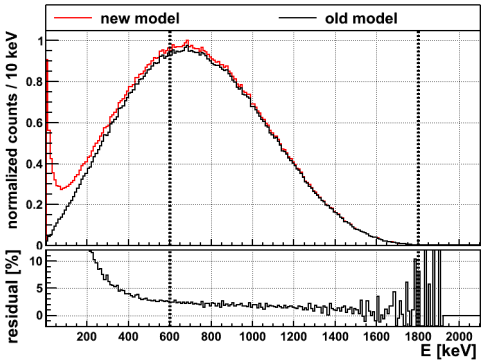

Figure 7. Energy spectrum of simulated $2\nu\beta\beta$ decays for new and old model.

For the $2\nu\beta\beta$ decay the active volume is increases when part of the n^+ electrode is semi-active compared to the old dead layer assumption. Applying the new model to $2\nu\beta\beta$ decays inside a typical detector results in a 2 % increase in active volume in the energy range of $600 - 1800$ keV [13]. In addition the spectral shape changes with the largest effects below 600 keV (Fig. 7). This region is however not accessible in GERDA due to the dominating background of ^{39}Ar (565 keV beta endpoint). The new n^+ model will help to increase the precision of future ^{76}Ge $2\nu\beta\beta$ decay half-life measurements which have a current precision of 5 % [3].

5. Conclusions

A new n^+ electrode model was developed from first principles based on diffusion of the charge carriers. This model was folded into Geant4 MC simulations and tuned and compared to calibration source measurements resulting in a good description of the data. The new model was applied to simulations of the dominating ^{42}K surface background predicting a suppression factor of up to 145. This is the first time that the large suppression of surface backgrounds is understood in detail. Additionally, the active volume and the spectral shape of $2\nu\beta\beta$ decays is

affected by the proper treatment of the n^+ electrode. The effective volume for $2\nu\beta\beta$ is increased by 2 % when including the semi-active layer, which reduces the $2\nu\beta\beta$ decay rate inferred from a measurement.

References

[1] K.-H. Ackermann et al. (GERDA Collaboration), Eur. Phys. J. C 73:2330 (2013).
[2] M. Agostini et al. (GERDA Collaboration), Phys. Rev. Lett. 111, 122503 (2013).
[3] M. Agostini et al. (GERDA Collaboration), Eur. Phys. J. C 75:416 (2015).
[4] M. Agostini et al. (GERDA Collaboration), Eur. Phys. J. C 73:2583 (2013).
[5] M. Agostini et al. (GERDA Collaboration), Eur. Phys. J. C 74:2764 (2014).
[6] B. Lehnert, Proceedings of the International School of Physics "Enrico Fermi", 182, 309 - 313 (2012).
[7] Canberra Semiconductor NV, Lammerdries 25, B-2439 Olen, Belgium.
[8] M. Agostini et al., J. Instr. 6 P03005 (2011).
[9] M. Agostini et al., J. Instr. 4 P10007 (2009).
[10] M. Agostini et al. (GERDA Collaboration), Eur. Phys. J. C 75:255 (2015).
[11] P. S. Finnerty, "A Direct Dark Matter Search with the Low-Background Broad Energy Germanium Detector", The University of North Carolina at Chapel Hill (2013).
[12] M. Agostini et al. (GERDA Collaboration), Eur. Phys. J. C 75:39 (2015).
[13] B. Lehnert, "Search for $2\nu\beta\beta$ Excited State Transitions and HPGe Characterization for Surface Events in GERDA Phase II", Dresden University of Technology (2016).
[14] M. Salathe, "Study on modified point contact germanium detectors for low background applications", Heidelberg University (2015).
[15] M. Boswell, Y.-D. Chan, and J. Detwiler et al., IEEE Trans. Nucl. Sci. 58 1212 (2011).